ChemComm

COMMUNICATION

View Article Online
View Journal | View Issue

Cite this: *Chem. Commun.*, 2025, **61**, 16842

Received 31st July 2025,
Accepted 17th September 2025

DOI: 10.1039/d5cc04356e

rsc.li/chemcomm

Controlling crystallisation with audible low frequency sound

Yasmin C. S. Figueiredo,[a] Thiago G. Tabuti,[a] Thaisa B. F. Moraes,[a] Julian Ticona-Chambi,[b] Rafael G. Candido,[a] Silvia L. Cuffini,[b] Marcelo S. Martins,[d] Walter L. M. Tupinambá,[d] Eduardo R. Triboni *[a] and Jonathan W. Steed *[c]

We show that low-frequency audible sound drives the crystallisation of distinct solid forms of organic compounds in solution crystallisation. In contrast to silent crystallisation, ROY and anthranilic acid crystallized as distinct polymorphs, concomitant forms, and with novel morphologies resulting in preferred orientation depending on the sound frequency and amplitude.

Audible low frequency sound (ALFS) in the range of 20–20 000 Hz is not expected to interfere directly with matter at atomic or molecular levels due to its long wavelengths. The usual ALFS outcomes are the occurrence of patterns over liquid surfaces and from materials which are spread upon plates, termed Chladni figures or Faraday instability.[1,2] However, there is evidence that ALFS can promote rearrangements and assemblies of molecules in solution,[3,4] regulate biological processes, and enhance the rate of crystallisation of proteins.[5,6] In addition, Wang and coworkers found a significant influence of ALFS on the redox-reaction of viologen molecules forming spatio-temporal patterns related to oxidation or reduction process.[7] Closely related studies have captured acoustic sounds derived from solution crystallisations and applying acoustic levitation to evaluate crystal growth.[8,9] ALFS differs from ultrasound because it is not expected to give rise to acoustic cavitation. Ultrasonic waves of frequencies between 20 kHz and 100 kHz and at sufficient amplitude can form and collapse microscopic bubbles within liquids,[10] delivering high thermal energy and shock waves which may provide sonochemically induced transformations as well as impact the assembly of molecules and macromolecules.[11,12] Hence, ultrasound has resulted in accelerated crystallization, controlled size distribution and morphology, and polymorphic outcome.[13–17] There are many crystallisation techniques such as antisolvent crystallisation, vapor diffusion, melt crystallisation, evaporation, cooling and rapid evaporation.[18,19] All of these approaches at a certain point create a supersaturation domain whereby molecules may nucleate and grow to bulk crystals. Upon crystallisation molecules may pack in distinct arrangements and conformations giving rise to the occurrence of polymorphs whose physicochemical properties such as melting point, solubility, electrical conductivity and colour can be significantly different from one another.[18–20] Such a structure–property relationship brings about the need for exhaustive screening looking for desired features, particularly for active pharmaceutical ingredients which have particular requirements for solubility, processing characteristics, and bioavailability. Herein, we have conceived an unprecedented ALFS crystallisation (sound crystallisation) technique based on the premise that ALFS passing through the crystallising solution may perturb and drive all stages of crystallisation, since it is an out-of-equilibrium process. To test this hypothesis we chose the popular 5-methyl-2-[(2-nitrophenyl)amino]thiophene-3-carbonitrile (**ROY**) as a model because it provides a range of colours and specific morphologies for each of its fourteen polymorphs including yellow prisms (Y), red prisms (R), orange needles (ON), orange plates (OP), yellow needles (YN), orange-red plates (ORP), and red plates (RP),[21–25] Fig. 1A. The seven most commonly accessible **ROY** polymorphs are stable at room temperature and crystallise from solvent-based processes, which leads to the occurrence of concomitant polymorphism.[26–28] A homemade acoustic apparatus comprising

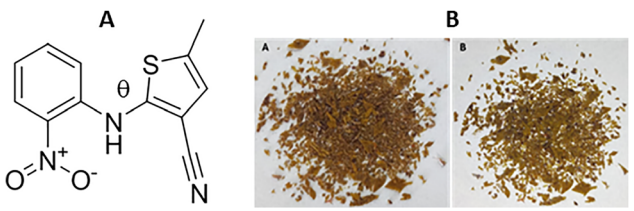

Fig. 1 (A) **ROY** torsion angle *q* between the aromatic rings accounts for different colours; (B) crystals of **ROY** form Y produced in silent crystallisations without ALFS from isopropanol (left) and from ethanol (right).

[a] *Laboratório Nanotecnologia e Engenharia de Processos-- NEP, Universidade de São Paulo, CEP 12602-810, Lorena, SP, Brazil. E-mail: tribonier@up.br*
[b] *Pós-graduação em Engenharia e Ciência de Materiais, Instituto de Ciência e Tecnologia (ICT), Universidade Federal de São Paulo (UNIFESP), São Paulo, Brazil*
[c] *Department of Chemistry, Durham University, South Road, Durham DH1 3LE, UK. E-mail: jon.steed@durham.ac.uk*
[d] *Departamento de Mecânica – Laboratório de Estruturas, Universidade Estadual Paulista, UNESP/FEG – Campus de Guaratinguetá, Brazil*

wave-generator, sub-woofer, amplifier, and an acrylic plate was built up for performing the **ROY** sound crystallisations. Crystallisations were performed in ethanol (EtOH) and isopropanol (i-Prop) and were found to give rise to concomitant forms, preferred orientation, and unexpected polymorphs depending upon the ALFS setup and the interplay of frequency, amplitude and solvent (see SI, Section SI-1 for experimental and sound standardisation details). In this work typical solvent-based crystallisation is termed 'silent crystallisation' and was carried out as a control in order to compare with crystallisation under ALFS conditions ('sound crystallisation'). Additionally, we extended the ALFS setup to crystallise anthranilic acid (AA) in water, giving rise to the unexpected form I in this solvent. To the best of our knowledge this is the first report of the use of ALFS for controlling the crystal characteristics of organic compounds and, hence, we anticipate that sound crystallisation may offer a new tool in solid form screening and control and may serve as key technique in process industries dealing with molecular crystallisation.

The silent **ROY** crystallisations in both EtOH and i-Prop gave rise to crystals with the same powdery appearance as the purchased material, Fig. 1B, and the powder X-ray diffraction (PXRD) patterns showed it to be the Y form (monoclinic, space group $P2_1/n$ – CSD refcode QAXMEH01,[29] SI-2). This polymorph has a torsion angle (θ) of 104.7° and its structure is dominated by π–π stacking of the nitrophenyl and thiophenyl substituents. This polymorph is the most stable polymorph in the solid state at room temperature.[30] Moreover, the Y polymorph is expected to nucleate in alcohols like MeOH, EtOH and i-Prop as well as the YN and OP **ROY** forms.[27,29] Sound crystallisation significantly modifies the crystal morphologies and colours of **ROY** samples depending upon the acoustic setup and whether the crystallisation vessel is either placed on the plate or simply hung on the subwoofer. This suspended arrangement is simply influenced by the acoustic field passing through it, whereas that settled on the plate must be seen as a mechanically coupled acoustic crystallisation because the whole system, *i.e.* vessel wall, plate, and subwoofer, is interconnected and vibrates as the sound parameters change. The suspended arrangement gave rise to the same Y polymorph as the silent procedures but with different crystal colours and preferred orientation depending mainly upon the solvent, but not significantly on the ALFS parameters. Dark yellow prisms (Fig. 2A, Y1) came out from ethanol while fibre-like structures were obtained from i-Prop (Fig. 2B, Y2) regardless of the amplitude or frequency used. Thermal analysis of these two solids shows very similar melting onset temperatures, 110.1 °C and 110.7 °C, respectively, for the prismatic- and fibre-like **ROY**, Fig. 2A and B; this difference is within experimental error. The pictures in Fig. 2 highlight the distinct appearance of the Y1 and Y2 **ROY** morphologies, and Fig. 3 shows the diffractogram of these solids after grinding. An SEM image of this needle-like structure is shown in detail (Fig. SI-3B). Combining ALFS and isopropanol, therefore, an unexpected morphology and hence preferred orientation arises for the Y form whose usual habit is prismatic. The morphology of the sound-crystallized **ROY** resembles the YN form (triclinic, space group $P\bar{1}$ – CSD QAXMEH04)[29] but PXRD analysis confirms it to be the thermodynamically stable Y polymorph (QAXMEH01). Hence, the ALFS induces a

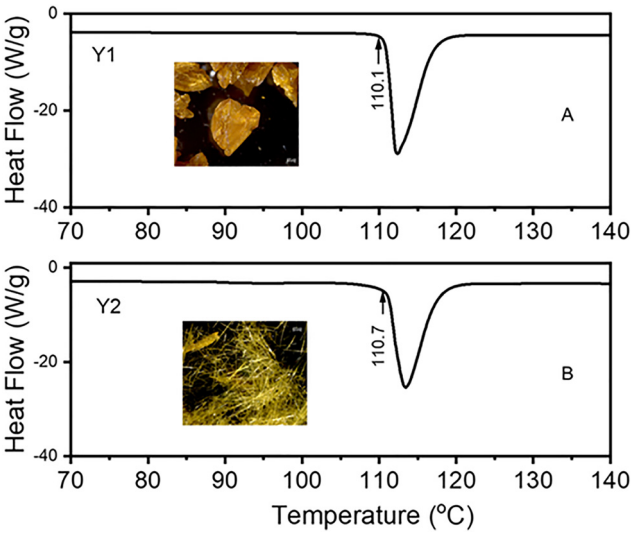

Fig. 2 DSC thermograms showing the melting onset of **ROY** crystals (polymorph Y) produced using ALFS crystallisation in suspended mode (A) Y1 and (B) Y2.

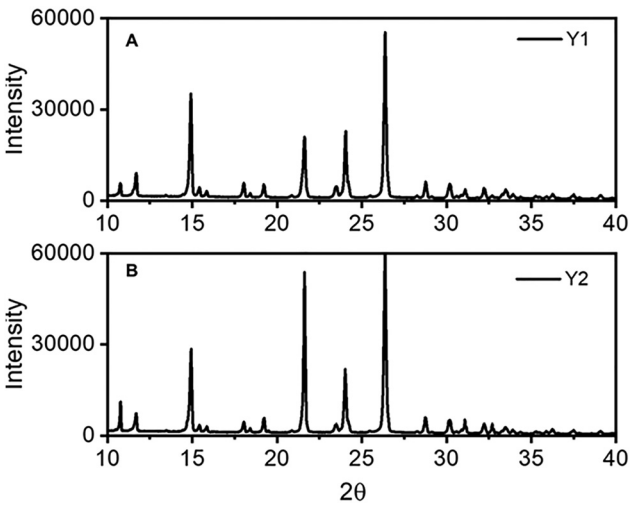

Fig. 3 PXRD of the **ROY** obtained by suspended ALFS crystallisation; (A) Y1 from EtOH, and (B) Y2 from i-Prop.

preferential growth of one of the facets of the Y crystal resulting in (010) preferred orientation (SI-3).

On the other hand, the mechanically coupled crystallisations were more sensitive to the ALFS parameters and to the solvents as well, providing a variety of **ROY** forms, Fig. 4A and B. In i-Prop at varying intensities of 80 dB, 90 dB, and 100 dB, and at frequencies of both 40 and 80 Hz, three different solid forms or mixtures were obtained, respectively: ON form (monoclinic, $P2_1/c$, CSD QAXMEH),[29] ON and Y concomitant forms, and the Y polymorph. In EtOH, however, distinct frequencies led to different results. At 40 Hz only the Y polymorph is formed when using 80 dB and 100 dB, whereas at 80 Hz the low amplitude delivers predominantly the ON polymorph while the high amplitude one the Y one. Fig. 5 depicts the diffractograms of pure **ROY** polymorphs ON and Y. The ON form is unexpected when

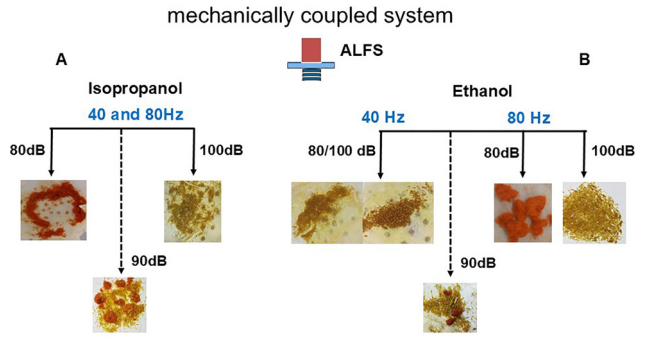

Fig. 4 Mechanically coupled crystallisations: (A) **ROY** polymorphs formed in isopropanol at different sound amplitudes regardless frequency, (B) **ROY** forms obtained in ethanol in which sound frequency and amplitude prove to be significant parameters; dashed lines indicate concomitant crystallisation.

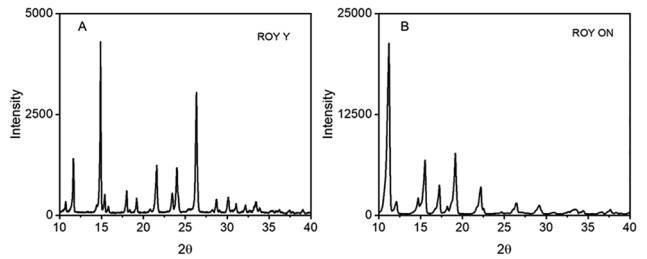

Fig. 5 Diffractograms of the **ROY**, (A) Y and (B) ON polymorphs obtained at different ALFS parameters.

crystallising in alcohols from which the most common form is the OP polymorph.[25] However, the most significant outcome is the selective crystallisation of **ROY** polymorphs as the amplitude is changed, and in ethanol different frequencies of 80 or 40 Hz nucleate distinct polymorphs. The tendency is at low intensity 80 dB the ON form is preferred over any other while at 100 dB the Y form is prevalent. Notably, at 90 dB, for all the ALFS parameters the two ON and Y forms always solidified out, hence resulting in consistent concomitant polymorphism (see PXRD and pictures of these solid forms in Section SI-4). These outcomes demonstrate a significant impact of ALFS on crystallisation result, whether just passing the wave through the solution or mechanically coupling it.

In order to rule our extraneous factors we measured the amount of evaporation and cooling rate of the solvents, as well as determined the possible water sorption under both ALFS and silent conditions for 60 min (SI-5). Fig. SI-5 shows temperatures obtained at different frequencies and amplitudes at 80 and 100 dB, and those for silent conditions. In all cases, the starting temperatures at 60 °C decrease by approximately half of their initial value after 10 min then drops smoothly to room temperature (at 22 °C), but the solutions remain around 2° to 4 °C warmer under ALFS than in silent mode. The solvent loss by evaporation averaged 0.7 mL for both silent and ALFS crystallisation systems and with no significant water uptake by Karl Fischer titration, indicating the same supersaturation regime during the crystallisation processes. Given that **ROY** crystallisation begins in a range of 5 to 10 min, and taking into account distinct results obtained by changing the ALFS parameters, we can rule out differences in the cooling, evaporation rate, and water absorption on the ALFS crystallisation results.

Anthranilic acid (AA, 2-aminobenzoic acid) has three known polymorphs.[30,31] Forms I and II (CSD refcodes AMBACO07 and AMBACO05)[32,33] are orthorhombic structures in space groups $P2_1cn$ and $Pbca$, while polymorph III adopts $P2_1/c$ (CSD AMBACO08).[34] Form I is a zwitterionic polymorph with one neutral and one ionic hydrogen bond in the asymmetric unit ($Z' = 2$), whereas forms II and III have the centrosymmetric carboxylic acid dimer synthon ($Z' = 1$).[31] Form I has been reported to crystallise from ethanol and methanol, and form II in protic polar and aprotic dipolar solvents as water, methanol, ethanol, acetic acid, acetonitrile and nitrobenzene mainly by using slow evaporation, whereas thermal techniques such as sublimation and melt crystallisation have been the best way to prepare form III.[30,31] Recently, Bag and coworkers obtained the kinetically crystallised form I from water by a fast evaporation technique that avoids conversion into the most stable form II.[30] We attempted to prepare AA polymorphs by mechanically coupled ALFS crystallisation in water at varying intensities of 80 dB and 100 dB, and at frequencies of 40 and 80 Hz. Single and concomitant crystallisation of forms I and II was observed depending on the ALFS configuration, and were confirmed by PXRD, Fig. 6. In addition, these polymorphs can be easily identified by their intrinsic solid-state fluorescence since form I exhibits a bright blueish colour while form II is off-white when exciting at $\lambda = 365$ nm, Fig. 7. Variation of the ALFS parameters provides distinct and opposite results. At 40 Hz, crystallisations performed at low (80 dB) and high (100 dB) amplitudes give rise, respectively, to form II and to the occurrence of concomitant polymorphs, with form I being quite prevalent. Conversely, at 80 Hz, form I crystallises out at low amplitude while form II is formed at high amplitude, with single polymorphs obtained in each case. Silent crystallisation in water leads to the expected form II.[32,33] Therefore, beyond driving a selective occurrence of two anthranilic acid polymorphs, sound crystallisation is allowing the crystallisation of the metastable form I in water.

Audible low frequency sound has a very significant effect on the solvent crystallisation of **ROY** and anthranilic acid and is likely to have a significant influence on the crystallisation outcomes of many substances including those of pharmaceutical interest. The results of both the suspended and mechanically coupled crystallisations gave rise to different polymorphs, influenced preferred orientation and resulted in concomitant

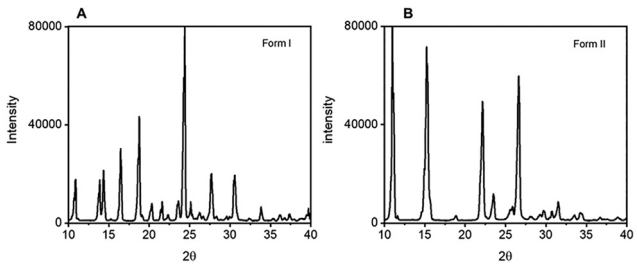

Fig. 6 PXRD of the AA crystals obtained by sound crystallisation; (A) diffractogram of the form I and (B) of the form II.[30]

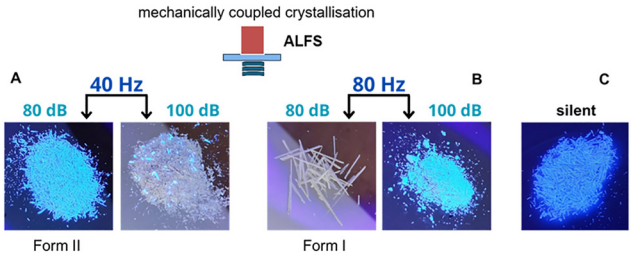

Fig. 7 Mechanically coupled crystallisations of the anthranilic acid in water: (A) at 40 Hz, form II formed at 80 dB and concomitant forms I and II at 100 dB, (B) at 80 Hz, form I obtained at 80 dB and form II at 100 dB.

crystallisation of multiple forms depending on the ALFS amplitude and frequency as well as the solvent. In the **ROY** crystallisation system, polymorphs ON and Y selectively crystallised out from ethanol and isopropanol, and an unusual needle-like morphology of Y was obtained in preference to the prismatic one in the suspended ALFS arrangement, resulting in pronounced preferred orientation. In the anthranilic acid system, both the forms I and II were selectively formed in water, hence, giving rise to the unexpected formation of the less stable form I which does not usually crystallise from water due to its conversion to the most stable form II. These results highlight the promising application of the ALFS on such out-of-equilibrium process although it remains very difficult yet to predict in advance which ALFS parameters will result in the crystallisation of a particular polymorph. Nevertheless, these results indicate that ALFS represents a potentially significant new crystallisation tool in the polymorph screening arsenal.

We thank the undergraduate Jonas Luis Massuchini de Carvalho from EEL-USP for the starting studies with **ROY** crystallisation supported by USP fellowship. The São Paulo Research Foundation – FAPESP grants 2021/01509-0, 2022/06346-5, 2024/09719-2 (ERT), 2019/27157-3 (TBFM). CAPES grant 88887.847777/2023-00 (TGT) and FINEP grant 012323700 (RGC).

Conflicts of interest

There are no conflicts to declare.

Data availability

Underlying research data for this paper is available from **https://doi.org/10.15128/r28k71nh14w**.

Supplementary information (SI): experimental details, PXRD pattern of ROY preferred orientation, author information. See DOI: **https://doi.org/10.1039/d5cc04356e**.

Notes and references

1 V. Zhou, K. Sariola, V. Latifi and V. Liimatainen, *Nat. Commun.*, 2016, 7(1), 12764.
2 M. T. Westra, D. J. Binks and W. Van De Water, *J. Fluid Mech.*, 2003, **496**, 1.
3 A. Tsuda, Y. Nagamine, R. Watanabe, Y. Nagatani, N. Ishii and T. Aida, *Nat. Chem.*, 2010, **2**, 977.
4 Y. S. Fukushima, J. Motoyanagi and A. Tsuda, *Chem. Commun.*, 2015, **51**, 2790.
5 C. Y. Zhang, Y. Wang, R. Schubert, Y. Liu, M. Y. Wang, D. Chen and D. C. Yin, *Cryst. Growth Des.*, 2016, **16**, 705.
6 C. Y. Zhang, J. Liu, M. Y. Wang, W. J. Liu, N. Jia, C. Q. Yang, M. L. Hu, Y. Liu, X. Y. Ye, R. B. Zhou and D. C. Yin, *Cryst. Growth Des.*, 2018, **19**, 258.
7 I. Hwang, R. D. Mukhopadhyay, P. Dhasaiyan, S. Choi, S. Y. Kim, Y. H. Ko and K. Kim, *Nat. Chem.*, 2020, **12**, 808.
8 S. B. Gregersen, M. J. Povey, M. D. Andersen, M. Hammershøj, M. Rappolt, A. Sadeghpour and L. Wiking, *Eur. J. Lipid Sci. Technol.*, 2016, **118**, 1257.
9 W. J. Xie, C. D. Cao, Y. J. Lü and B. Wei, *Phys. Rev. E*, 2002, **66**, 061601.
10 K. S. Suslick, *Science*, 1990, **247**, 1439.
11 W. Chen, P. Dai, C. Hong, C. Zheng, W. Wang and X. Yan, *Cryst. Eng. Commun.*, 2018, **20**, 2989.
12 J. Liu, G. Song, Y. Yuan, L. Zhou, D. Wang, T. Yuan and J. Gong, *Ultrason. Sonochem.*, 2022, **86**, 106025.
13 A. Kozell, A. Solomonov and U. Shimanovich, *FEBS Lett.*, 2023, **597**, 3013.
14 K. A. Ramisetty, A. B. Pandit and P. R. Gogate, *Ind. Eng. Chem. Res.*, 2013, **52**, 17573.
15 Q. Zhao, L. Yang, C. Yao and G. Chen, *Ind. Eng. Chem. Res.*, 2023, **62**, 20083.
16 P. R. Birkin, J. J. Youngs, T. T. Truscott and S. Martini, *Phys. Chem. Chem. Phys.*, 2022, **24**, 11552.
17 J. R. Sander, B. W. Zeiger and K. S. Suslick, *Ultrason. Sonochem.*, 2014, **21**, 1908.
18 A. Myerson, *Handbook of Industrial Crystallisation*, Butterworth-Heinemann, 2022.
19 J. W. Steed and J. L. Atwood, *Supramolecular Chemistry*, John Wiley & Sons, 2022.
20 J. Bernstein, *Polymorphism in Molecular Crystals*, International Union of Crystal, 2020.
21 A. J. Alvarez, A. Singh and A. S. Myerson, *Cryst. Growth Des.*, 2009, **9**, 4181.
22 A. Nangia, *Acc. Chem. Res.*, 2008, **41**, 595.
23 S. Chen, I. A. Guzei and L. Yu, *J. Am. Chem. Soc.*, 2005, **127**, 9881.
24 A. Levesque, T. Maris and J. D. Wuest, *J. Am. Chem. Soc.*, 2020, **142**, 11873.
25 G. J. Beran, I. J. Sugden, C. Greenwell, D. H. Bowskill, C. C. Pantelides and C. S. Adjiman, *Chem. Sci.*, 2022, **13**, 1288.
26 A. R. Tyler, R. Ragbirsingh, C. J. McMonagle, P. G. Waddell, S. E. Heaps, J. W. Steed and M. R. Probert, *Chem*, 2020, **6**, 1755.
27 T. Gnutzmann, Y. Nguyen Thi, K. Rademann and F. Emmerling, *Cryst. Growth Des.*, 2014, **14**, 6445.
28 P. T. Cardew and R. J. Davey, *Cryst. Growth Des.*, 2019, **19**, 5798.
29 L. Yu, *Acc. Chem. Res.*, 2010, **43**, 1257.
30 M. Tan, A. G. Shtukenberg, S. Zhu, W. Xu, E. Dooryhee, S. M. Nichols and Q. Zhu, *Faraday Discuss.*, 2018, **211**, 477.
31 L. Yu, G. A. Stephenson, C. A. Mitchell, C. A. Bunnell, S. V. Snorek, J. J. Bowyer and S. R. Byrn, *J. Am. Chem. Soc.*, 2000, **122**, 585.
32 P. P. Bag and C. M. Reddy, *Cryst. Growth Des.*, 2012, **12**, 2740.
33 S. S. Kumar and A. Nangia, *Cryst. Growth Des.*, 2014, **14**, 1865.
34 C. J. Brown and M. Ehrenberg, *Acta Crystallogr., Sect. C: Cryst. Struct. Commun.*, 1985, **41**, 441.